

A Convolutional Perfectly Matched Layer (CPML) for the Fourth-Order One-Step Leapfrog HIE-FDTD Method

Mian Dong, Juan Chen, and Anxue Zhang

School of Electrical and Information Engineering
Xi'an Jiaotong University, Xi'an 710049, People's Republic of China
Chen.juan.0201@mail.xjtu.edu.cn

Abstract — A new convolutional perfectly matched layer (CPML) for the fourth-order one-step leapfrog hybrid implicit explicit finite-difference time-domain (HIE-FDTD) method for the TE case has been proposed in this paper. When the time step size satisfies with the time stability condition, the maximum reflection error of the proposed method is below -72dB, which demonstrates good absorbing performance of the CPML method. To verify the accuracy and efficiency of the proposed method, we compare the results of the traditional FDTD method and the HIE-FDTD method. Numerical examples demonstrate that the proposed method consumes about 60.13% less CPU time than the traditional FDTD method and 41.60% less CPU time than the existing HIE-FDTD method.

Index Terms — Accuracy, computational efficiency, convolutional perfectly matched layer (CPML), fourth order one-step leapfrog, hybrid implicit and explicit-FDTD (HIE-FDTD), relative reflection error.

I. INTRODUCTION

The finite-difference time-domain (FDTD) [1] method has been proven to be an effective means that provides accurate predictions of field behaviours for varieties of electromagnetic iteration problems. However, as it is based on an explicit finite-difference algorithm, the Courant-Friedrich-Levy (CFL) condition [2] must be satisfied when this method is used. In order to remove the CFL limit, many improved methods have been developed.

In 1999, the alternating direction implicit FDTD (ADI-FDTD) method was proposed in [3-5]. The time-step size in the ADI-FDTD technique was no longer constrained by the CFL limit and could be any value theoretically. However, the accuracy of the ADI-FDTD method is constrained by the numerical dispersion [6] and the splitting error associated with the square of the time step size [7-8]. Besides, it must solve six tridiagonal matrices and six explicit updates for one whole update cycle, which makes the ADI-FDTD method computationally inefficient. In 2005, a locally-one-

dimension FDTD (LOD-FDTD) method was proposed in [9], [10]. The LOD-FDTD method requires less arithmetic operations than the ADI-FDTD method while providing comparable accuracy [10]. In 2006, a hybrid implicit and explicit-FDTD (HIE-FDTD) method was proposed in [11-14]. The time-step size of the HIE-FDTD method is determined by two space discretization. The HIE-FDTD method is weakly conditionally stable and is extremely useful for problems with very fine structures in one direction. Afterwards, a one-step leapfrog HIE-FDTD scheme has been proposed in [15] with its field updated in the same manner as that of the traditional FDTD method. Recently, a fourth-order leapfrog HIE-FDTD method was proposed in [16]. The method not only has the second-order accurate in time and the fourth-order accurate in space, but also has the one-step leapfrog schemes. Therefore, the method spend much less computational time and got better accuracy. However, up to now, such an efficient fourth-order one-step leapfrog HIE-FDTD method with absorbing boundary conditions (ABCs) hasn't been studied systematically.

In this paper a new convolutional perfectly matched layer (CPML) for the fourth-order one-step leapfrog HIE-FDTD method [17] is proposed. The time stability of the proposed method is $\Delta t = 6\Delta x/7c$ [18]. Numerical examples demonstrate that the proposed method has very high accuracy and efficiency. What's more, when the time step size satisfies with the time stability condition, the maximum reflection error of the proposed method is below -72dB, which demonstrates good absorbing performance of the CPML method. For simplicity, the two-dimensional (2-D) fourth-order one-step leapfrog HIE-CPML update equations are discussed in this paper. The formulations for a 3-D fourth-order HIE-FDTD method can be developed following a similar procedure.

The organization of this paper is as follows. In Section 2, the formulations of proposed algorithm are presented. The absorbing performance with CPML of proposed method is presented in Section 3. The numerical results applied to validate the efficiency and the accuracy of the proposed method, the traditional

FDTD method and the existing HIE-FDTD method are presented in Section 4.

II. FORMULATION

The numerical formulations of the two-dimensional fourth-order one-step leapfrog HIE-FDTD method proposed in [16] are presented as follows:

$$\begin{cases} E_x^n = E_x^{n-\frac{1}{2}} + \frac{\Delta t}{2\varepsilon} \delta_y H_z^{n-\frac{1}{2}} \\ E_y^n = E_y^{n-\frac{1}{2}} - \frac{\Delta t}{2\varepsilon} \delta_x H_z^{n-\frac{1}{2}} \\ H_z^n = H_z^{n-\frac{1}{2}} + \frac{\Delta t}{2\mu} \left(\delta_y E_x^{n-\frac{1}{2}} - \delta_x E_y^n \right) \end{cases}, \quad (1)$$

$$\begin{cases} E_x^{n+\frac{1}{2}} = E_x^n + \frac{\Delta t}{2\varepsilon} \delta_y H_z^{n+\frac{1}{2}} \\ E_y^{n+\frac{1}{2}} = E_y^n - \frac{\Delta t}{2\varepsilon} \delta_x H_z^{n+\frac{1}{2}} \\ H_z^{n+\frac{1}{2}} = H_z^n + \frac{\Delta t}{2\mu} \left(\delta_y E_x^{n+\frac{1}{2}} - \delta_x E_y^n \right) \end{cases}, \quad (2)$$

$$\begin{cases} E_x^{n+1} = E_x^{n+\frac{1}{2}} + \frac{\Delta t}{2\varepsilon} \delta_y H_z^{n+\frac{1}{2}} \\ E_y^{n+1} = E_y^{n+\frac{1}{2}} - \frac{\Delta t}{2\varepsilon} \delta_x H_z^{n+\frac{1}{2}} \\ H_z^{n+1} = H_z^{n+\frac{1}{2}} + \frac{\Delta t}{2\mu} \left(\delta_y E_x^{n+\frac{1}{2}} - \delta_x E_y^{n+1} \right) \end{cases}. \quad (3)$$

The CPML [18] is an efficient implementation of the complex frequency-shifted (CFS) constitutive PML parameters, originally proposed by Kuzuoglu and Mittra to introduce a strictly causal form of the PML. The modified Maxwell's equations in the CPML region can be written as [18-19]:

$$\begin{cases} \frac{\partial E_x}{\partial t} = \frac{1}{\varepsilon} \left(\frac{1}{k_y} \frac{\partial H_z}{\partial y} + \psi_{xy} \right) \\ \frac{\partial E_y}{\partial t} = \frac{1}{\varepsilon} \left(\frac{1}{k_x} \frac{\partial H_z}{\partial x} + \psi_{yx} \right) \\ \frac{\partial H_z}{\partial t} = \frac{1}{\varepsilon} \left(\frac{1}{k_y} \frac{\partial E_x}{\partial y} - \frac{1}{k_x} \frac{\partial E_y}{\partial x} + \psi_{hzy} - \psi_{hzx} \right) \end{cases}, \quad (4)$$

where ψ is the auxiliary term related to the field quantities in the CPML, and k_x , k_y are nonnegative real numbers, respectively.

Here,

$$\begin{aligned} \psi_{xy}^{n+1/2} &= b_y \psi_{xy}^{n-1/2} + a_y \delta_y H_z^{n+1/2}, \\ \psi_{yx}^{n+1/2} &= b_x \psi_{yx}^{n-1/2} + a_x \delta_x H_z^{n+1/2}, \end{aligned}$$

$$\psi_{hzy}^{n+1} = b_y \psi_{hzy}^{n+1} + a_y \delta_y E_x^n,$$

$$\psi_{hzx}^{n+1} = b_x \psi_{hzx}^{n+1} + a_x \delta_x E_y^n,$$

$$b_\xi = e^{-\left(\frac{\sigma_\xi + \alpha}{k_\xi} \right) \left(\frac{\Delta t}{\xi}\right)}, \quad a_\xi = \frac{\sigma_\xi}{\sigma_\xi k_\xi + k_\xi^2 \alpha} (b_\xi - 1),$$

$$\sigma_\xi = \frac{\sigma_{\max} |\xi - \xi_0|^m}{d^m}, \quad \sigma_{\max} = (m+1) / (150\pi \Delta_\xi),$$

$$k_\xi = 1 + (k_{\max} - 1) \frac{|\xi - \xi_0|^m}{d^m}, \quad \xi = x, y.$$

Here α and a_ξ are assumed to be nonnegative real number and ξ_0 is the position of the CPML layer. d and σ_{\max} are the thickness of the CPML in x and y directions and the maximum conductivity, respectively. m and Δ_ξ are the cell size and the order of polynomial scaling, respectively. For these simulations, the value of m is chosen as 4.

By applying the CPML layer to (1)-(3), a set of time marching equations is derived and expressed as follows:

$$E_x^n = E_x^{n-\frac{1}{2}} + \frac{\Delta t}{2\varepsilon} \left\{ \frac{\delta_y}{k_y} H_z^{n-\frac{1}{2}} + \psi_{exy}^{n-\frac{1}{2}} \right\}, \quad (5-1)$$

$$E_y^n = E_y^{n-\frac{1}{2}} - \frac{\Delta t}{2\varepsilon} \left\{ \frac{\delta_x}{k_x} H_z^{n-\frac{1}{2}} + \psi_{eyx}^{n-\frac{1}{2}} \right\}, \quad (5-2)$$

$$H_z^n = H_z^{n-\frac{1}{2}} - \frac{\Delta t}{2\mu} \left\{ \frac{\delta_y}{k_y} E_x^{n-\frac{1}{2}} - \frac{\delta_x}{k_x} E_y^{n-\frac{1}{2}} + \psi_{hzy}^{n-\frac{1}{2}} - \psi_{hzx}^n \right\}, \quad (5-3)$$

$$E_x^{n+\frac{1}{2}} = E_x^n - \frac{\Delta t}{2\varepsilon} \left\{ \frac{\delta_y}{k_y} H_z^{n+\frac{1}{2}} + \psi_{exy}^{n+\frac{1}{2}} \right\}, \quad (6-1)$$

$$E_y^{n+\frac{1}{2}} = E_y^n - \frac{\Delta t}{2\varepsilon} \left\{ \frac{\delta_x}{k_x} H_z^{n+\frac{1}{2}} + \psi_{eyx}^{n+\frac{1}{2}} \right\}, \quad (6-2)$$

$$H_z^{n+\frac{1}{2}} = H_z^n - \frac{\Delta t}{2\mu} \left\{ \frac{\delta_y}{k_y} E_x^{n+\frac{1}{2}} - \frac{\delta_x}{k_x} E_y^n + \psi_{hzy}^{n+\frac{1}{2}} - \psi_{hzx}^n \right\}, \quad (6-3)$$

$$E_x^{n+1} = E_x^{n+\frac{1}{2}} + \frac{\Delta t}{2\varepsilon} \left\{ \frac{\delta_y}{k_y} H_z^{n+\frac{1}{2}} + \psi_{exy}^{n+\frac{1}{2}} \right\}, \quad (7-1)$$

$$E_y^{n+1} = E_y^{n+\frac{1}{2}} - \frac{\Delta t}{2\varepsilon} \left\{ \frac{\delta_x}{k_x} H_z^{n+\frac{1}{2}} + \psi_{eyx}^{n+\frac{1}{2}} \right\}, \quad (7-2)$$

$$H_z^{n+1} = H_z^{n+\frac{1}{2}} - \frac{\Delta t}{2\mu} \left\{ \frac{\delta_y}{k_y} E_x^{n+\frac{1}{2}} - \frac{\delta_x}{k_x} E_y^{n+\frac{1}{2}} + \psi_{hzy}^{n+\frac{1}{2}} - \psi_{hzx}^n \right\}. \quad (7-3)$$

Substituting (5-3) into (5-1), we have:

$$\begin{aligned} E_x^n &= \left(1 - \frac{\Delta t^2 \delta_y^2}{4\varepsilon \mu k_y^2} \right) E_x^{n-\frac{1}{2}} + \frac{\Delta t^2}{4\varepsilon \mu} \frac{\delta_x \delta_y}{k_x k_y} E_y^n \\ &+ \frac{\Delta t^2 \delta_y}{4\varepsilon \mu k_y} \left(\psi_{hzx}^n - \psi_{hzy}^{n-\frac{1}{2}} \right) + \frac{\Delta t}{2\varepsilon} \left(\frac{\delta_y}{k_y} H_z^n + \psi_{exy}^{n-\frac{1}{2}} \right). \end{aligned} \quad (8)$$

By substituting (6-3) and (8) into (6-1), the updating equation for E_x^n is obtained as follows:

$$\begin{aligned} & \left(1 - \frac{\Delta t^2 \delta_y^2}{4\epsilon\mu k_y^2}\right) \left(E_x^{n+\frac{1}{2}} - E_x^{n-\frac{1}{2}}\right) \\ &= \frac{\Delta t \delta_y}{2\epsilon k_y} H_z^n + \frac{\Delta t}{2\epsilon} \left(\psi_{exy}^{n+\frac{1}{2}} + \psi_{exy}^{n-\frac{1}{2}}\right). \end{aligned} \quad (9)$$

In Eq. (9), it often uses the finite difference to approximate the spatial derivate [20], [21]. For example:

$$\begin{aligned} & \frac{\partial f(x, y, t)}{\partial x} \Big|_{x=i\Delta x}^{n+\frac{1}{2}}, \\ & \approx \frac{1}{\Delta x} \sum_{h=0}^{H-1} \alpha(h) \left[f \Big|_{i+h+\frac{1}{2}, j}^{n+\frac{1}{2}} - f \Big|_{i-h-\frac{1}{2}, j}^{n+\frac{1}{2}} \right], \end{aligned} \quad (10)$$

where $\alpha(h)$ can be obtained as follows [22]:

$$\alpha(h) = \frac{(-1)^h}{2\left(h + \frac{1}{h}\right)^2} \frac{((2H-1)!)^2}{(2H-2-2h)!(2H+2h)!}.$$

When H is equal to 2, the order of the algorithm is equal to 4. According to the definition of the constant $\alpha(h)$ and by substituting (10) into (9), then introducing the auxiliary variable e and h as indicated in [23], i.e.,

$$\begin{aligned} e_m^{n+1/2} &= E_m^{n+1/2} - E_m^{n-1/2} \dots \text{in } x, y, \\ e_m^{n+1} &= H_m^{n+1} - H_m^n \dots \text{in } x, y. \end{aligned}$$

The final updating equations of $E_x^{n+1/2}$ of the proposed method can be finally obtained as follows,

$$\begin{aligned} & c_1 e_x \Big|_{i+1/2, j}^{n+1/2} - c_2 \left(e_x \Big|_{i+1/2, j+1}^{n+1/2} - e_x \Big|_{i+1/2, j-1}^{n+1/2} \right) \\ & - c_3 \left(e_x \Big|_{i+1/2, j+2}^{n+1/2} - e_x \Big|_{i+1/2, j-2}^{n+1/2} \right) \\ & - c_4 \left(e_x \Big|_{i+1/2, j+3}^{n+1/2} - e_x \Big|_{i+1/2, j-3}^{n+1/2} \right), \quad (11) \\ & = c_5 \left(H_z \Big|_{i+1/2, j+1/2}^n - H_z \Big|_{i+1/2, j-1/2}^n \right) \\ & - c_6 \left(H_z \Big|_{i+1/2, j+3/2}^n - H_z \Big|_{i+1/2, j-3/2}^n \right) \\ & + c_7 \left(\psi_{exy} \Big|_{i+1/2, j}^{n+1/2} - \psi_{exy} \Big|_{i+1/2, j}^{n-1/2} \right) \end{aligned}$$

where

$$\begin{aligned} c_1 &= \frac{365\Delta t^2}{576\epsilon\mu\Delta y^2}, c_2 = \frac{87\Delta t^2}{256\epsilon\mu\Delta y^2}, \\ c_3 &= \frac{3\Delta t^2}{128\epsilon\mu\Delta y^2}, c_4 = \frac{\Delta t^2}{2304\epsilon\mu\Delta y^2}, \\ c_5 &= \frac{9\Delta t}{8\epsilon\mu\Delta y}, c_6 = \frac{\Delta t}{24\epsilon\mu\Delta y}, c_7 = \frac{\Delta t}{2\epsilon}. \end{aligned}$$

The other updating equations of the proposed method

can be obtained similarly and are not shown here for simplicity.

III. ABSORBING PERFORMANCE

In order to study the absorbing performance of the CPML absorbing boundary, the relative reflection error of the fourth-order one-step leapfrog HIE-CPML method is discussed. A simulation of sinusoidally modulated Gaussian pulse as an input electric current profile is studied. The time dependence of the excitation function is as follows:

$$s(t) = \exp\left(-\frac{(t-t_0)^2}{\tau^2}\right) \sin(2\pi f_0(t-t_0)), \quad (12)$$

where f_0 , t_0 and τ are constants. Here, we choose $f_0 = 5\text{GHz}$, and $t_0 = \tau = 6 \times 10^{-10}\text{s}$. This excitation source is used throughout the paper A 3.0GHz i5 professor PC with 8GHz memory is used to calculate the results. In the all simulation, the relative reflection error is defined as follows:

$$E_{ror} = 20 \log_{10} \left| \frac{E_y(t) - E_{y,ref}(t)}{E_y(t)} \right|. \quad (13)$$

where $E_y(t)$ is the time-dependent electric field at the observation point calculated by using the proposed method truncated by the CPML. $E_{y,ref}(t)$ represents the reference electric field and is measured at the same observation point by extending the dimensions of the computation domain to 500×500 grids so that the reflected wave does not return at the observation point before the simulation was not terminated. It can almost avoid any possible reflection effect from boundaries. The CPML constructive parameters for these simulations are $k_{\max} = 12$, $\alpha = 0.07$ [24].

The relation between the relative reflection errors of the proposed method and the variable α is presented in Fig.1. The spatial step sizes in this simulation are $\Delta_x = 0.006$ and $\Delta_y = 0.0006$. The time step size of the proposed method is $\Delta t = 6\Delta x/7c = 17.14\text{ps}$. It can be seen from the Fig. 1 that the proposed method with CPML absorbing boundary has different relative reflection errors as α takes different values. When the value of α is larger than 0.07, the maximum relative reflection error is less than -72dB. However, when the value of α is less than 0.07, the relative errors deteriorate so that the maximum relative reflection error would reach to -51dB. Therefore, the optimal value of α is equal to 0.07. With this value, the relative reflection error of the HIE-FDTD method is below -72.52dB in the entire simulation history.

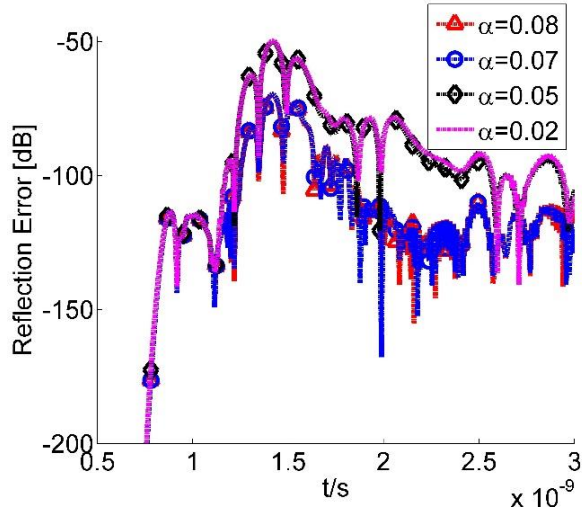


Fig. 1. The relation between the relative reflection errors and the order of the polynomial α .

In order to present relations between the relative reflection error and the time step size of the proposed method, the variation of the relative reflection error with respect to different CFLN values is presented in Fig. 2. Here, the value of the α is equal to 0.07. Figure 2 shows that as the increase of the CFLN, the relative reflection error of the proposed method increases gradually. Even when CFLN takes its maximum value, namely, CFLN=8.657, the relative reflection error still can reach to -51.45dB, which shows excellent absorbing performance of the CPML.

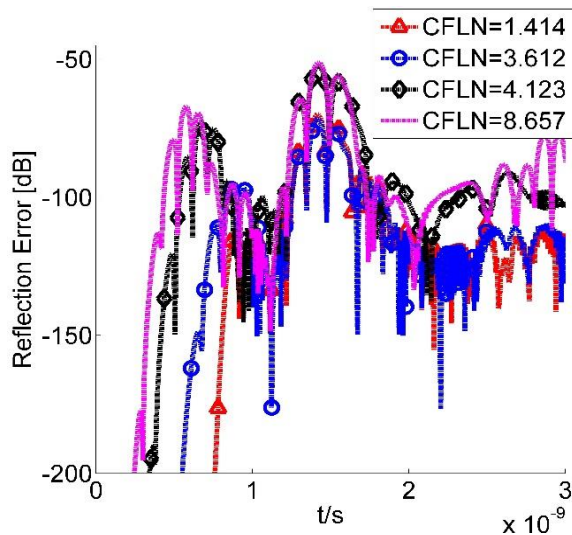


Fig. 2. The relation between the relative reflection errors and the CFLN value.

Next, it is instructive to observe the relation between the maximum reflection error and the CPML constructive

parameters k_{\max} , σ_{\max} . Figure 3 illustrates the contour curves of the maximum relative reflection error against k_{\max} , σ_{\max} at the observation point. It is demonstrated from the Fig. 3 that the best absorbing performance can be achieved in a larger range by selected the values of k_{\max} and σ_{\max} effectively. That makes it easy to predict the optimal values. Obviously, when $k_{\max}=12$ and $\sigma_{\max}=\sigma_{\text{opt}}=1$, the maximum errors of the proposed method can reach to -72dB.

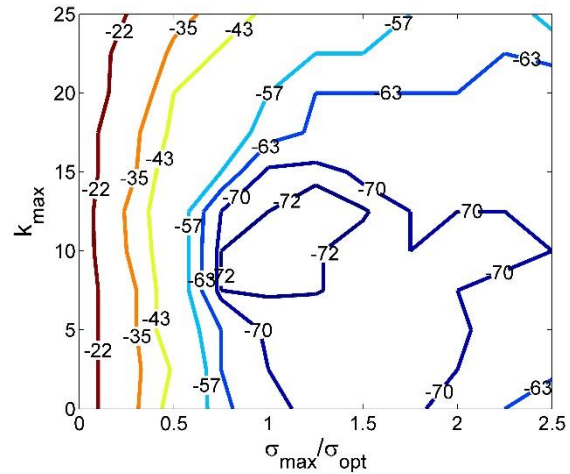


Fig. 3. The maximum relative reflection error at observation point as a function.

IV. ACCURACY AND EFFICIENCY

To validate the accuracy and efficiency of presented algorithm, a simulation of sinusoidally modulated Gaussian pulse as an input electric current profile is studied. A 2-D computational domain with the dimension $84\text{cm} \times 8.4\text{cm}$ is shown in Fig. 4. The computational domain is free space and is discretized with $\Delta_x = 0.006$ and $\Delta_y = 0.0006$ respectively. The total lattice dimension is 140×140 . The current source is placed at the centre of the domain and the observation point $p1$ is placed 30cm away from the source. Ten cell-thick CPML layers are used to terminate the computational domain [23].

Applied the traditional FDTD method, the HIE-FDTD method [24-25] and the proposed method to compute the field components at the observation point, the results are shown in Fig. 5. The time-step sizes in the three methods are $\Delta t = 1 / \left(c \sqrt{1/\Delta x^2 + 1/\Delta y^2} \right) = 1.99\text{ps}$,

$$\Delta t = 1 / \left(c \sqrt{1/\Delta x^2} \right) = 20.10\text{ps} \text{ and } \Delta t = 6\Delta x/7c = 17.14\text{ps},$$

respectively. They are the maximum time-step size of each method to satisfy the time stability condition. It can be seen from the Fig. 5 that the component calculated by

using the proposed method agrees very well with the results calculated by using the traditional FDTD method and the HIE-FDTD method, which demonstrates the proposed method has a high accuracy.

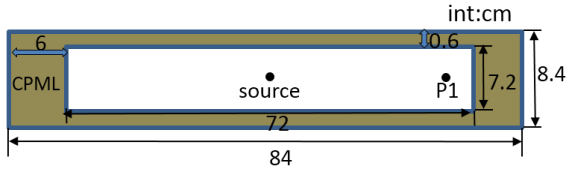


Fig. 4. Free space truncated by CPML.

In order to study the efficiency of the proposed method, more simulations are presented here. The time-step size of the traditional FDTD method is chosen as $\Delta t = 1.990 ps$. In the HIE-FDTD method, they are chosen as $\Delta t = 1.99, 3.98, 7.96, 17.14 ps$ and in the proposed method, they are also $\Delta t = 1.99, 3.98, 7.96, 17.14 ps$. To complete these simulations, the computational times of these methods are presented in Table 1. The numbers of the computational iterations of each method are also

presented in the Table 1.

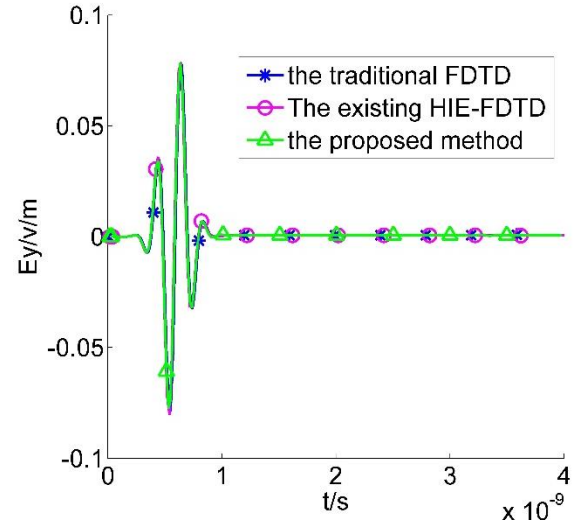


Fig. 5. The electric field values at p_1 calculated by the FDTD algorithm, the existing HIE-FDTD algorithm and the proposed HIE-FDTD algorithm.

Table 1: Computer costs of the FDTD algorithm, the HIE-FDTD algorithm and the proposed method

Δt (ps)		1.99=1.99*1	3.98=1.99*2	7.96=1.99*4	17.14=1.99*8.6
CFLN		1	2	4	8.6
The traditional FDTD	Number of iterations	2000			
	CPU time (s)	29.1			
The HIE-FDTD	Number of iterations	2000	1000	500	232
	CPU time (s)	171.0	84.9	42.7	19.8
The proposed method	Number of iterations	2000	1000	500	232
	CPU time (s)	101.3	50.2	25.1	11.6

As shown in Table 1, when CFLN is 8.6, the proposed method consumes about 60.13% less CPU time than the traditional FDTD method. The main reason is as follows: the time-step size of the proposed method is 8.6 times larger than that of the traditional FDTD method. Therefore, the iteration number is much smaller for the same simulated time history. Besides, compared with the HIE-FDTD method, the proposed method saves about 41.60% CPU time, although the time step size in these two methods are same. This is because the formulation of the proposed method is much conciser than the HIE-FDTD method. It means even the proposed method uses same time-step size as the HIE-FDTD method, its computational time considerably reduced compared with that of the HIE-FDTD method. Note that if CFLN=1 is used, the proposed method would have no advantages over the traditional FDTD method. As the computational time of each iteration is longer because of additional efforts needed for solving the tri-diagonal linear system in proposed method.

VI. CONCLUSION

This paper introduces the CPML absorbing boundary conditions theories into the fourth-order one-step leapfrog HIE-FDTD algorithm. It is found that the technique is weakly conditionally stable and supports time step size greater than the CFL limit. Numerical simulations show that the maximum reflection error as low as -72 dB can be achieved by selecting $k_{\max} = 12$ and $\sigma_{\max}/\sigma_{opt} = 1.0$. It demonstrates the proposed method with CPML has good absorbing performance. Besides, the field components calculated by using the proposed method agree very well with the result calculated by using the traditional FDTD method and the HIE-FDTD method, which indicates that the proposed method has excellent calculation accuracy and low computational error. What's more, the computer cost of the proposed algorithm is much less than the traditional FDTD algorithm and the HIE-FDTD method. It means the proposed algorithm has higher efficiency.

ACKNOWLEDGMENT

This work was supported by National Natural Science Foundations of China (No. 61231003, 61601360, 61501365 and 61471292), and also supported by the Fundamental Research Funds for the Central Universities.

REFERENCE

- [1] K. S. Yee, "Numerical solution of initial boundary value problems involving Maxwell's equations in isotropic media," *IEEE Transactions on Antennas Propagation*, vol. 14, pp. 302-307, 1996.
- [2] A. Taflove, *Computational Electrodynamics*. Norwood, MA: Artech House, 1995.
- [3] T. Namiki, "A new FDTD algorithm based on alternating-direction implicit method," *IEEE Trans. Microwave Theory Tech.*, vol. 47, pp. 2003-2007, 1999.
- [4] Q.-X. Chu, L.-N. Wang, and Z.-H. Chen, "A novel numerical dispersion formulation of the 2D ADI-FDTD method," *International Journal of RF and Microwave Computer-Aided Engineering*, vol. 16, no. 6, pp. 584-587, 2006.
- [5] X.-T. Zhao, Z.-G. Wang, and X.-K. Ma, "A 3-D unconditionally stable precise integration time domain method for the numerical solutions of Maxwell's equations in circular cylindrical coordinates," *International Journal of RF and Microwave Computer-Aided Engineering*, vol. 19, no. 2, pp. 230-242, 2009.
- [6] H. X. Zheng and K. W. Leung, "An efficient method to reduce the numerical dispersion in the ADI-FDTD," *IEEE Trans. Microwave Theory Tech.*, vol. 53, pp. 2295-2301, 2005.
- [7] S. Wang and C. W. Trueman, "An iterative ADI-FDTD with reduced splitting error," *IEEE Microw. Compon. Lett.*, vol. 15, pp. 92-94, 2005.
- [8] J. Chen and J. Wang, "Error between unconditionally stable FDTD methods and conventional FDTD method," *Electron. Lett.*, vol. 42, pp. 1132-1133, 2006.
- [9] V. E. Nascimento, F. L. Teixeira, and B. H. V. Borges, "Unconditionally stable finite-difference time-domain method based on the locally-one-dimensional technique," *Proc. 22nd Symp. Brasileiro Telecomun.*, vol. 9, pp. 288-291, 2005.
- [10] J. Shibayama, M. Muraki, J. Yamauchi, et al., "Efficient implicit FDTD algorithm based on locally one-dimensional scheme," *Electron. Lett.*, vol. 41, pp. 1046-1047, 2005.
- [11] B. Huang and G. Wang, "A hybrid implicit-explicit FDTD scheme with weakly conditional stability," *Microwave Opt. Technol. Lett.*, vol. 39, pp. 97-101, 2003.
- [12] J. Chen and J. Wang, "A 3-D hybrid implicit-explicit FDTD scheme with weakly conditional stability," *Microwave Opt. Technol. Lett.*, vol. 48, pp. 2291-2294, 2006.
- [13] J. Chen and J. G. Wang, "A three-dimensional semi-implicit FDTD scheme for calculation of shielding effectiveness of enclosure with thin slots," *IEEE Transactions on Electromagnetic Compatibility*, vol. 49, pp. 354-360, 2007.
- [14] J. Chen and J. G. Wang, "Numerical simulation using HIE-FDTD method to estimate various antennas with fine scale structures," *IEEE Transactions on Antennas Propagation*, vol. 55, pp. 3603-3612, 2007.
- [15] J. Wang, B. Zhou, L. Shi, C. Gao, et al., "A novel 3-D HIE-FDTD method with one-step leapfrog scheme," *IEEE Trans. Microw. Theory Tech.*, vol. 62, pp. 1275-1283, 2014.
- [16] M. Dong, A. Zhang, and J. Chen, "The fourth order one-step leapfrog HIE-FDTD method," *Applied Computational Electromagnetics Society Journal*, vol. 31, pp. 1370-1376, 2016.
- [17] D.-W. Zhu, Y.-G. Wang, and H.-L. Chen, "A one-step leapfrog HIE-FDTD method for rotationally symmetric structures," *International Journal of RF and Microwave Computer-Aided Engineering*, 2016.
- [18] J. A. Roden and S. D. Gedney, "Convolutional PML (CPML): An efficient FDTD implementation of the CFS-PML for arbitrary media," *Microw. Opt. Technol. Lett.*, vol. 27, pp. 334-339, 2002.
- [19] M. Krumpholz and L. P. B. Katehi, "MRTD: New time-domain schemes based on multiresolution analysis," *IEEE Trans. Microwave Theory Tech.*, vol. 44, pp. 555-571, 1996.
- [20] M. L. Ghrist, "High order difference methods for wave equations," *University of Colorado*, 1997.
- [21] S. C. Yang, Z. Chen, Y. Yu, et al., "The unconditionally stable one-step leapfrog ADI-FDTD method and its comparisons with other FDTD methods," *IEEE Microw. Wireless Compon. Lett.*, vol. 21, pp. 640-642, 2011.
- [22] S. D. Gedney, "The perfectly matched layer absorbing medium," *Advances in Computational Electrodynamics: The Finite Difference Time Domain*, A. Taflove (Editor), Artech House, Boston, MA, pp. 263-340, 1998.
- [23] J. Wang, Y. Wang, and D. Zhang, "Truncation of open boundaries of cylindrical waveguides in 2.5-dimensional problems by using the convolutional perfectly matched layer," *IEEE Trans. Plasma Sci.*, vol. 34, pp. 681-690, 2006.
- [24] J. Chen, N. Xu, and A. Zhang, "Using dispersion HIE-FDTD method to simulate the graphene-based polarizer," *IEEE Transaction on Antennas and Propagation*, vol. 24, pp. 3011-3017, 2016.
- [25] J. Chen and J. Wang, "Three-dimensional dispersive hybrid implicit-explicit finite-difference time-domain method for simulations of graphene," *Computer Physics Communications*, vol. 207, pp. 211-216, 2016.